



# Inferring Late-stage Enrichment of Exoplanet Atmospheres from Observed Interstellar Comets

Darryl Z. Seligman<sup>1</sup> , Juliette Becker<sup>2</sup> , Fred C. Adams<sup>3,4</sup> , Adina D. Feinstein<sup>5,6</sup> , and Leslie A. Rogers<sup>5</sup> <sup>1</sup>Department of the Geophysical Sciences, University of Chicago, Chicago, IL 60637, USA; [dzseligman@uchicago.edu](mailto:dzseligman@uchicago.edu)<sup>2</sup>Division of Geological and Planetary Sciences, California Institute of Technology, Pasadena, CA 91125, USA<sup>3</sup>Physics Department, University of Michigan, Ann Arbor, MI 48109, USA<sup>4</sup>Astronomy Department, University of Michigan, Ann Arbor, MI 48109, USA<sup>5</sup>Department of Astronomy and Astrophysics, University of Chicago Chicago, IL 60637, USA

Received 2022 April 15; revised 2022 June 1; accepted 2022 June 14; published 2022 June 29

## Abstract

The discovery of the first two interstellar objects implies that, on average, every star contributes a substantial amount of material to the galactic population by ejecting such bodies from the host system. Because scattering is a chaotic process, a comparable amount of material should be injected into the inner regions of each system that ejects comets. For comets that are transported inwards and interact with planets, this Letter estimates the fraction of material that is accreted or outward-scattered as a function of planetary masses and orbital parameters. These calculations indicate that planets with escape velocities smaller than their current-day orbital velocities will efficiently accrete comets. We estimate the accretion efficiency for members of the current census of extrasolar planets and find that planetary populations including but not limited to hot and warm Jupiters, sub-Neptunes, and super-Earths can efficiently capture incoming comets. This cometary enrichment may have important ramifications for postformation atmospheric composition and chemistry. As a result, future detections and compositional measurements of interstellar comets will provide direct measurements of material that potentially enriched a subpopulation of the extrasolar planets. Finally, we estimate the efficiency of this enrichment mechanism for extrasolar planets that will be observed with the James Webb Space Telescope (JWST). With JWST currently operational and these observations imminently forthcoming, it is of critical importance to investigate how enrichment from interstellar comet analogs may affect the interpretations of exoplanet atmospheric compositions.

*Unified Astronomy Thesaurus concepts:* [Interstellar objects \(52\)](#); [Exoplanet atmospheres \(487\)](#); [Comets \(280\)](#); [Chemical enrichment \(580\)](#)

## 1. Introduction

Planetary enrichment from comet collisions is a process that has been extensively studied—and even observed in real time—in the solar system. In 1993, the comet Shoemaker–Levy 9 was discovered (Shoemaker et al. 1993) and within a year it collided with Jupiter (Weaver et al. 1995). Observations of the Jovian atmosphere during and immediately following the collision revealed the presence of molecules that had never previously been detected there, including carbonyl sulfide and carbon monosulfide (Lellouch et al. 1995; Noll et al. 1995). More generally, previous work has estimated that the late heavy bombardment (LHB) would have enriched Jupiter and Saturn with mass increments of  $0.15 \pm 0.04 M_{\oplus}$  and  $0.08 \pm 0.01 M_{\oplus}$  from comets (Matter et al. 2009).

While the accretion of Shoemaker–Levy 9 was a historical astronomical event, it is not representative of the fate of typical solar system comets. Short-period comets (SPCs), or ecliptic comets with low inclinations, originate in the Kuiper Belt and are subsequently perturbed onto orbits interior to the orbit of Neptune (Leonard 1930; Edgeworth 1943; Kuiper 1951; Fernandez 1980; Duncan et al. 1988; Quinn et al. 1990). They temporarily reside in the Centaur region on giant-planet-crossing

orbits until they reach the inner solar system and become Jupiter Family Comets (JFCs) (Hahn & Bailey 1990; Levison & Duncan 1997; Tiscareno & Malhotra 2003; Di Sisto & Brunini 2007; Bailey & Malhotra 2009; Di Sisto et al. 2009; Nesvorný et al. 2017; Fernández et al. 2018; Seligman et al. 2021a). Because the escape velocity of Jupiter is larger than its orbital velocity, close encounters with the giant planet typically scatter comets back into the Centaur region or into the inner solar system, instead of resulting in a collision. In most models of the solar system’s formation, these scattering events with giant planets undergoing radial migration and/or instability ejected tens of Earth masses worth of comets into interstellar space (Hahn & Malhotra 1999; Gomes et al. 2004; Morbidelli et al. 2005; Tsiganis et al. 2005; Levison et al. 2008; Raymond et al. 2020).

The discovery of the first two interstellar objects, 1I/‘Oumuamua and 2I/Borisov, confirmed that the ejection of planetesimals is a ubiquitous process. Although a variety of ejection mechanisms have been proposed, their relative importance remains unclear. The net result is the production of a galactic population of interstellar objects with a spatial number density of  $n_o \sim 0.1\text{--}0.2 \text{ au}^{-3}$  (Jewitt et al. 2017; Laughlin & Batygin 2017; Trilling et al. 2017; Do et al. 2018; Moro-Martín 2018; Zwart et al. 2018; Moro-Martín 2019; Levine et al. 2021). One promising ejection mechanism is simple ejection via interactions with giant planets (Laughlin & Batygin 2017; Raymond et al. 2018; Zhang & Lin 2020). Alternative scenarios include ejection from a stellar system exhibiting post-main-sequence evolution (Hansen & Zuckerman 2017;

<sup>6</sup> NSF Graduate Research Fellow.



Rafikov 2018) and from a circumbinary system (Ćuk 2018; Jackson et al. 2018).

Because scattering is a chaotic process, the amount of material scattered inward should be roughly comparable to that ejected in systems that produce interstellar comets. This balance implies that the population of interstellar comets is representative of the cometary bodies that are delivered from the exterior to the interior in nascent planetary systems. As a result, extrasolar planets that are capable of efficiently accreting comets can potentially experience significant chemical enrichment and atmospheric erosion from this population (Wyatt et al. 2020). Because compositional ratios and metallicities of planetary atmospheres are often believed to contain signatures of their formation locations (Öberg et al. 2011), this cometary enrichment mechanism may have nonnegligible ramifications for interpreting observations of exoplanet atmospheres.

The compositions of interstellar comets are thus representative of the material that potentially enriched extrasolar planets. For example, 2I/Borisov had more CO than H<sub>2</sub>O, and these two molecules were the dominant constituents of its volatile inventory (Bodewits et al. 2020; Cordiner et al. 2020). The composition of ‘Oumuamua was not measured because no coma was detected (Jewitt et al. 2017; Meech et al. 2017; Trilling et al. 2018). Based on the object’s nongravitational acceleration (Micheli et al. 2018), however, it is plausible that it was composed primarily of H<sub>2</sub> (Füglister & Pfenniger 2018; Seligman & Laughlin 2020; Levine & Laughlin 2021), N<sub>2</sub> (Desch & Jackson 2021; Jackson & Desch 2021), or CO (Seligman et al. 2021b).

This present work investigates the process of cometary enrichment of exoplanet atmospheres implied by the existence of interstellar comets. This Letter is organized as follows. In Section 2, we calculate the efficiency with which a planet accretes comets as a function of its orbital and physical properties. In Section 3, we identify currently known exoplanets that are susceptible to cometary enrichment through this mechanism. In Section 4, we discuss the ramifications for upcoming observations of exoplanetary atmospheres with JWST and summarize our findings.

## 2. Efficiency of Cometary Accretion

When comets from the exterior regions in a planetary system are transported inwards by gravitational perturbations, they will eventually cross the orbits of the planets. These comets can then either be accreted by the planet through collisions or outwardly scattered. In this section, we estimate the fraction of comets that will collide with a planet as a function of its orbit and its planetary and stellar properties. At the end of this section, we discuss the cases when comets persist in the inner system without being accreted or ejected.

First, we clarify some terminology that will be used in the remainder of this Letter. The term “outward-scattering” colloquially encompasses both (i) scattering that leads the comet to remain in the system with changed orbital parameters, and (ii) scattering that ejects the comet from the system. For the remainder of this Letter, we only use the term outward-scattering to describe (ii). The initial events that perturb the comet onto a high-eccentricity trajectory toward the interior of the planetary system are referred to as inward transportation.

We consider a planet with mass  $M_p$ , radius  $R_p$ , semimajor axis  $a_p$ , and eccentricity  $e_p = 0$ . The comet is transported inward from a distant orbit and has semimajor axis  $a_c$  and

eccentricity  $e_c$ . The cross section of the planet that will lead to accretion,  $\sigma_A$ , is given by

$$\sigma_A = f_g (\pi R_p^2), \quad (1)$$

where  $f_g$  is a gravitational focusing factor defined as

$$f_g = 1 + \left( \frac{2GM_p}{R_p v_\infty^2} \right). \quad (2)$$

The relative speed of the comet when it crosses the orbit of the planet is proportional to the quantity  $\sqrt{3 - T}$ , where  $T$  is the Tisserand parameter with respect to the planet (Carusi et al. 1990). The Tisserand parameter with respect to a planet is approximately conserved during a close encounter, and is given by

$$T = \frac{a_p}{a_c} + 2 \sqrt{\frac{a_c}{a_p}} \sqrt{1 - e_c^2} \cos(i_c), \quad (3)$$

where  $i_c$  is the inclination of the comet. Because we consider comets with low  $i_c$ ,  $\cos i_c \approx 1$ . Therefore, the asymptotic velocity  $v_\infty$  in the frame of the giant planet is given by the expression

$$v_\infty^2(a_c, e_c) = \frac{GM_*}{a_p} \times \left( 3 - \frac{a_p}{a_c} - 2 \sqrt{\frac{a_c}{a_p}} \sqrt{1 - e_c^2} \right), \quad (4)$$

where  $M_*$  is the mass of the star. Comets with significant inclination have larger relative velocities and do not necessarily interact with the planet at perihelia. Moreover,  $a_c(1 - e_c^2) = p_c(1 + e_c)$ , where  $p_c$  is the periastron of the comet. Equation (4) relies on the assumption that the orbit of the planet and the comet are in the same plane. This assumption is reasonable because the ecliptic comets in the solar system typically have low inclination.

Because the comets are transported inward from the distant parts of the planetary system and the giant planets of interest reside at small to moderate semimajor axes, we assume that  $a_p \ll a_c$ . As a result, the eccentricity of the orbit of the comets must be large (close to unity), so that they cross the orbits of the planets on nearly radial trajectories. Equation (4) can be approximated as

$$v_\infty^2(a_c, e_c) \simeq \Lambda \left( \frac{GM_*}{a_p} \right), \quad (5)$$

where the coefficient  $\Lambda$  is defined to be

$$\Lambda = 3 - 2 \sqrt{\frac{p_c}{a_p}} \sqrt{1 + e_c}. \quad (6)$$

In the limiting case of high-eccentricity comets that barely intersect the orbit of the planet, where  $e_c \simeq 1$  and  $p_c = a_p$ , the coefficient  $\Lambda \simeq 3 - 2\sqrt{2}$ . Alternatively, if the comet would collide with the star on first approach and  $p_c \ll a_p$ , then  $\Lambda \simeq 3$ . Therefore, for the comets considered in this Letter,  $\Lambda \in (0.18, 3)$ . As a result, the gravitational focusing factor is given by

$$f_g \simeq 1 + \left( \frac{2M_p a_p}{\Lambda M_* R_p} \right), \quad (7)$$

and the cross section for accretion has the form

$$\sigma_A = \pi R_P^2 \left( 1 + \frac{2M_P a_P}{\Lambda M_* R_P} \right). \quad (8)$$

In order to eject the comet out of the system, the escape velocity from the planet at the distance of closest approach  $r$  must be greater than the escape velocity from the star system—which is related to the orbital velocity of the planet. This condition (which is necessary but not sufficient) can be written in the form

$$\frac{GM_P}{r} \geq \frac{GM_*}{a_P}. \quad (9)$$

We define the quantity  $R_S$  to be the distance of closest approach to the planet that is required in order to scatter the object out of the planetary system. In other words, for outward-scattering to occur, we must have  $r \leq R_S$ , where

$$R_S = \Gamma \frac{M_P a_P}{M_*}, \quad (10)$$

where  $\Gamma$  is a dimensionless factor of order unity. An analogous result arises from the requirement that the impact parameter for outward-scattering must be comparable to the semimajor axis of the hyperbolic orbit of the comet around the planet (e.g., see the discussion of Napier et al. 2021).

In order to calculate the fraction of objects that collide, out of all the objects that interact with the planet, we compare the relative cross sections for accretion and outward-scattering. We denote the Safronov number by  $\Theta$ , which is typically defined as

$$\Theta = \frac{M_P a_P}{M_* R_P}. \quad (11)$$

The two cross sections can then be written in the (approximate) forms

$$\begin{cases} \sigma_A \simeq \pi R_P^2 (1 + 2\Theta/\Lambda) \\ \sigma_S \simeq \pi R_P^2 (\Gamma^2 \Theta^2). \end{cases} \quad (12)$$

The ratio of the number of comets accreted by the planet to the number of comets that experience strong gravitational interactions with the planet (getting sufficiently close that they could be ejected from the system) is given by the ratio of the cross sections,  $\sigma_A/\sigma_S$ . We denote this ratio as the accretion efficiency  $\mathcal{A}$ , which is given by

$$\mathcal{A} = \min[1, (1 + 2\Theta/\Lambda)/(\Gamma^2 \Theta^2)]. \quad (13)$$

When  $\Theta \ll 1$ , the  $\sigma_A/\sigma_S$  given by Equation (12) can be much greater than unity. In this case, all comets that are sufficiently close to interact with the planet will be accreted. We set  $\mathcal{A} = 1$  with the min function in Equation (13) in this case.

This fraction only applies to comets that have (i) a planet-crossing orbit and (ii) a close encounter (within the outward-scattering cross section) at some point in time. These criteria guarantee that the comet experiences significant gravitational perturbations. However, the occurrence rate of these close encounters is low—of order the ratio of the diameter of the maximum of the two cross sections  $\sigma_A$  and  $\sigma_S$  to the orbital circumference—even for a comet with a planet-crossing orbit and low inclination. Nevertheless, the typical period of these cometary orbits,  $P_C$ , will be approximately  $P_C \leq 10^2 - 10^3$  yr. For typically evolved planetary systems, the comets will thus

orbit many times and will eventually experience close approaches to the planets.

It is feasible that the mechanism that initially transported comets into the interior of the system was significantly different than those that produce ecliptic comets in the solar system. In this case, some of the comets may have nonnegligible inclinations, making accretion by a planet less common. Specifically, when  $\pi (\sin(i_C) p_C)^2 > \text{Max}[\sigma_A, \sigma_S]$ , the comet will typically not interact with the planet at perihelia. Similarly, we have assumed an initial distribution of eccentricities for the scattered comets that eventually produce planet-crossing orbits. However, the distribution of eccentricities will also depend on the transport mechanism. Depending on the mechanism, a significant fraction of material could have periastrons that are too high to reach the outermost planet under consideration and contribute to enrichment. It is also possible that any given close approach might not result in ejection or accretion, and the comet is simply perturbed outside of the cross-sectional area. However, because of the differences in cometary orbit timescales and system ages, these comets are likely to (eventually) interact with a planet again.

A significant complication to this enrichment mechanism arises due to the finite lifetimes of the comets, commonly referred to as cometary fading. This process results primarily from volatile mass loss and less commonly from disintegration after multiple perihelia passages (Di Sisto et al. 2009; Brasser & Wang 2015). Typical mass-loss rates from an active nuclear surface area are of order  $\sim 40 \text{ g cm}^{-2}$  per perihelia passage of  $\sim 2 \text{ au}$  (Fernández 2005). However, the active fraction of the surface likely decreases with each perihelia passage (Fernández 2005). In the solar system, once an object becomes a JFC,<sup>7</sup> the average dynamical lifetime is  $\sim 12,000$  yr (Levison & Duncan 1997). Unfortunately, the efficiency of cometary fading remains unconstrained in (i) other planetary systems and (ii) for different types of comets. Nevertheless, it is possible that a substantial fraction of the comets (or fragments) that enrich a planet are severely depleted in surface volatiles. However, subsurface volatiles in cometary nuclei may remain intact indefinitely.

In Figure 1, we show the ratio of accreted to outward-scattered comets, given by Equation (13), as a function of the planetary Safronov number. The dashed and solid lines correspond to the limiting cases of  $\Lambda = 3 - 2\sqrt{2}$  and  $\Lambda = 3$ , and  $\Gamma = 1$ . For a given distribution of cometary eccentricities, the integrated accretion efficiency will be between these two curves. For both cases, this fraction falls quite steeply. As a leading-order approximation, Jovian planets interior to  $\sim 1 \text{ au}$  will experience enrichment from all comets that they interact with. When  $\Theta$  is large, the fraction of comets accreted is proportional to  $\Theta^{-1} \propto a^{-1}$ , for fixed values of the planet and host-star properties. This figure may be compared with Figures 1–4 in Wyatt et al. (2017), who performed a similar analysis accounting for the more general cases of cometary accretion, ejection, or retention for a range of stellar masses, planet masses, and semimajor axes and reached similar conclusions.

For example, WASP-77 Ab would have accreted all of the comets that it encountered, while the directly imaged massive planet HR 8799 b would have outward-scattered  $\sim 10^2 - 10^3$  times as many comets as it accreted. Interestingly, the

<sup>7</sup> A common definition of a JFC is an object with a Tisserand parameter with respect to Jupiter  $2 < T_J < 3$  (Levison 1996). See Table 1 in Seligman et al. (2021a) for an exhaustive list of literature definitions.



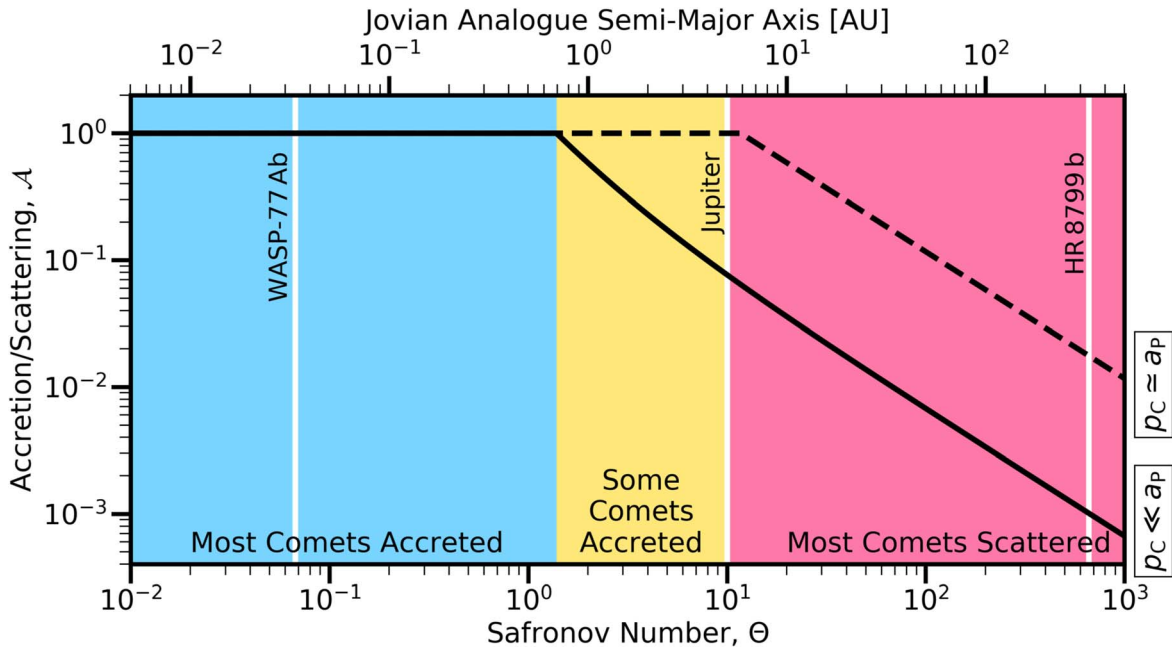


**Figure 1.** The ratio of accreted to outward-scattered comets, given by Equation (13), as a function of the Safronov number of the interacting planet. The (i) dashed and (ii) solid lines correspond to comets with perihelia (i) much less than ( $\Lambda = 3$ ,  $\Gamma = 1$ ) and (ii) approximately equal to ( $\Lambda = 0.18$ ,  $\Gamma = 1$ ) the semimajor axis of the scattering planet. The blue, yellow, and red regions indicate where  $\sigma_A/\sigma_C = 100\%$ ,  $10\% < \sigma_A/\sigma_C < 100\%$ , and  $\sigma_A/\sigma_C < 10\%$  for  $\Lambda = 3$ . The top  $x$ -axis shows the semimajor axis corresponding to the Safronov number on the bottom axis, for a planet with a Jovian mass and radius, orbiting a solar-type star. The positions of WASP-77 Ab, Jupiter, and HR 8799 b are indicated by vertical white lines.

atmospheric carbon-to-oxygen ratio of both of these planets has been measured to be  $0.59 \pm 0.08$  with a solar value of 0.55 (Line et al. 2021) and  $0.578 \pm 0.005$  (Ruffio et al. 2021) with a solar value of  $0.54_{-0.09}^{+0.12}$  (Wang et al. 2020), respectively. However, Line et al. (2021) also measured a subsolar overall metallicity in WASP-77 Ab. This suggests that the planet did not experience significant cometary enrichment, which may be due to the lack of external planets in the system.

Similarly, while the accretion efficiency for Jupiter is between 10% and 100%, Matter et al. (2009) calculated that the planet only accreted  $0.15 \pm 0.04 M_{\oplus}$  of material during the LHB. In their simulations, the primordial belt had  $24 M_{\oplus}$  of planetesimals when the instability that led to the LHB occurred. Our analytic calculation would predict Jupiter’s accretion of  $\sim 1 M_{\oplus}$  of planetesimals, which is inconsistent with the simulations by a factor of  $\sim 10$ . This may be due to (i) outward-scattering events with Saturn, Neptune, and Uranus and/or (ii) the initial distribution of eccentricities of the planetesimals inward-scattered by Neptune (see the discussion regarding eccentricity distribution in Section 4). Both of these examples demonstrate that numerical calculations should be applied when investigating this enrichment mechanism for specific planetary systems.

### 3. Cometary Enrichment of Exoplanets

The detections of ‘Oumuamua and Borisov imply that, on average, every star ejects approximately  $M_C \sim 1\text{--}10 M_{\oplus}$  of material into the galaxy (Laughlin & Batygin 2017). Because scattering is a highly chaotic process, a comparable amount of material should be scattered inwards as well, averaged across a large number of systems.

In exoplanet-hosting systems, cometary material with orbits perturbed strongly enough by this process to be placed onto planet-crossing orbits will eventually pass within a planetary interaction cross section. The final fate of the comet (accretion

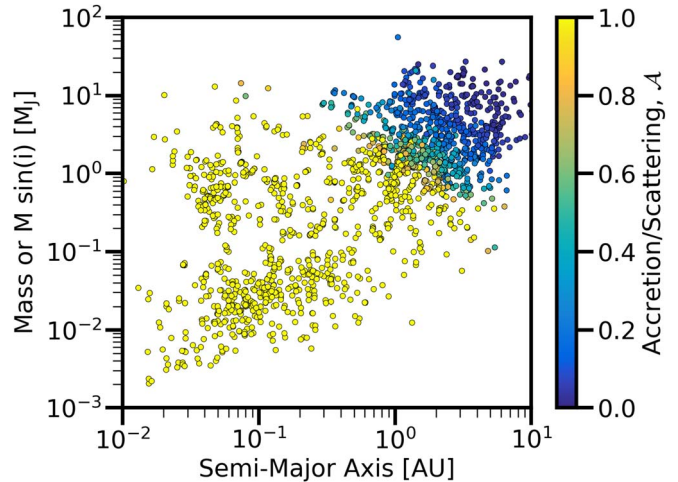


**Figure 2.** The cometary accretion efficiency for every detected exoplanet. The  $x$ -axis shows the orbital semimajor axis, and the  $y$ -axis shows the mass or  $m \sin i$  for each planet. The color of each point indicates the efficiency with which the planet accretes comets, as given by the ratio of the accretion to the outward-scattering cross section. We calculate this quantity using Equation (13) with  $\Lambda = 1$  and  $\Gamma = 1$ .

or ejection) is approximately set by the ratio of  $\sigma_A/\sigma_S$ . Exoplanets with  $\sigma_A/\sigma_S \sim 1$  potentially experienced significant postformation envelope enrichment from this population of comets. In Figure 2, we show this accretion efficiency for detected exoplanets. For planets that do not have measured radii, we approximate it using the empirical mass–radius relationship from Chen & Kipping (2017). It is evident that hot and warm Jupiters, sub-Neptunes, and super-Earths are efficient at accreting comets that they encounter. The population of Jovian mass planets with semimajor axes  $a > 1$  au tend to have higher Safronov numbers and accrete a lower fraction

of the cometary material that they experience close encounters with.

Therefore, compositions of interstellar comets may be representative of a fraction of the metal content of hot and warm Jupiters, super-Earths, and sub-Neptunes. Assuming that the injected mass is  $\sim M_C$  for every star, then multiplying this quantity by the fraction  $\sigma_A/\sigma_S$  in Figure 2 will yield an upper limit on the mass of cometary material from this population that was accreted by any planet—assuming that every inward-scattered comet experienced a close encounter with the planet. It is possible that additional cometary material was accreted, but this value of  $M_C$  corresponds only to the material that is directly analogous to the galactic population of interstellar comets.

This result provides an upper limit because our order-of-magnitude calculation does not take into account additional complications in the simplistic picture. In addition to the complications discussed in Section 2, one complication is that if there are multiple planets within a system, the comets will likely enrich the outermost planet that still has  $\sigma_A/\sigma_S \sim 1$ . A second complication is that while  $M_C \sim 1\text{--}10M_\oplus$  is estimated as an average value of material ejected per star, it is likely that the contributions from individual stellar systems vary. Moreover, some fraction (or even a significant fraction for some cases in Figure 1) of the inwardly transported comets are ejected in subsequent outward-scattering events. This effect can be reduced if inner planets have shorter scattering timescales (Wyatt et al. 2017), as confirmed with  $N$ -body simulations by Marino et al. (2018). Generally speaking, tightly packed low-mass planets were found to be more efficient at scattering material inward. These ejections would then also contribute to the interstellar comet population—effectively reducing the initial flux of inwardly transported material needed to match that implied by 1I/‘Oumuamua and 2I/Borisov. This effect would typically be less than a factor of  $\sim 2$  and within the uncertainties of this order-of-magnitude calculation. This interpretation implicitly relies on the assumption that the majority of enrichment occurs after the planet reaches its currently observed location. This requires planetary migration to occur early.

Atmospheric enrichment may also occur early ( $\tau \leq 10^7$  yr) via planetesimal accretion in situ (Zhou & Lin 2007; Shibata & Ikoma 2019; Podolak et al. 2020) or during migration (Shibata et al. 2020, 2022). It may be possible to distinguish between planetesimal and comet accretion based on the typical compositions of these objects. Their compositions are a function of formation location relative to various volatile condensation fronts (Öberg et al. 2011; Seligman et al. 2022). As an example, the atmospheric alkali metal content of hot Jupiters may indicate planetesimal accretion exterior to the  $\text{H}_2\text{O}$  snow line and subsequent inward migration (Hands & Helled 2022). The population-level compositions of interstellar comets are unconstrained, although 2I/Borisov exhibited a volatile C/O ratio indicative of formation exterior to the CO snow line (Bodewits et al. 2020; Cordiner et al. 2020; Seligman et al. 2022). If most interstellar comets form at large radial distances, interstellar cometary analogs, and planetesimals may deliver volatile material with varying condensation temperatures. However, the effects of cometary fading discussed earlier in this section may further complicate this picture.

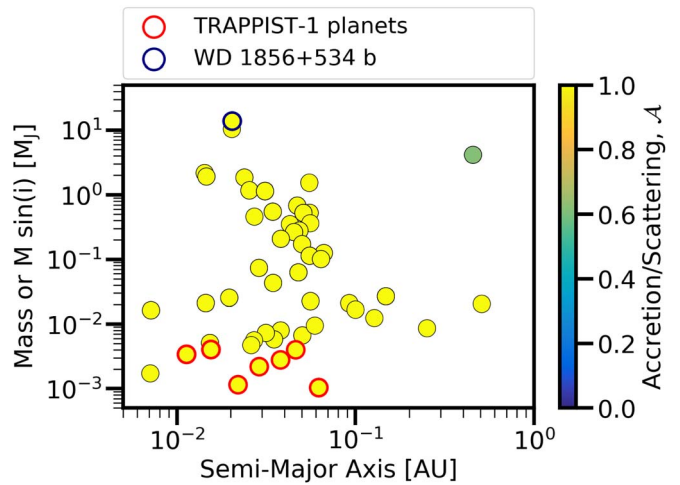


**Figure 3.** The accretion efficiency for exoplanets that will be observed with JWST. Because most targets are susceptible to cometary enrichment, this process should be considered when interpreting forthcoming observations of these exoplanetary atmospheres. We calculate this using Equation (13) with  $\Lambda = 1$  and  $\Gamma = 1$ . Note that the following JWST targets are not included in the figure: TOI-836 b TOI-836 c, TOI-175 b, GJ 341 b, GJ 4102 b, and TOI-134 b.

#### 4. Ramifications for Upcoming JWST Observations

In this Letter, we showed that hot Jupiters, warm Jupiter, sub-Neptunes, and super-Earths potentially experienced chemical enrichment from the accretion of a population of comets analogous to the interstellar comets. If every star, on average, ejected  $M_C \sim 1\text{--}10M_\oplus$  of material in interstellar comets then a comparable amount of material should also be transported inwards. Therefore, exoplanets that are capable of efficient accretion may have experienced significant enrichment from these comets.

This process could have important ramifications for observations of exoplanet atmospheres, especially with JWST operational. For example, the atmospheric carbon-to-oxygen ratio is believed to trace the formation location of giant planets (Öberg et al. 2011). However, this ratio could be significantly affected by cometary enrichment of up to  $M_C \sim 10M_\oplus$  of metals. In Figure 3 we show the same diagnostic of accretion efficiency as in Figure 2 for every planet that will be observed by JWST. It appears that almost every JWST target is susceptible to significant cometary enrichment. We highlight the TRAPPIST-1 planets, which may have experienced both atmospheric destruction and subsequent replenishment from cometary accretion (Kral et al. 2018).

However, due to the nonexhaustive list of complications discussed in the previous sections, the effects of this enrichment may be diminished for some or all of these planets. Importantly, the fraction of comets with planet-crossing orbits,  $\mathcal{F}$ , is determined by the eccentricity distribution produced by the inward-scattering process and  $a_p$ . A flat eccentricity distribution results in  $\mathcal{F} \simeq a_p/a_C \simeq 1/40$ . If the distribution is steeper or shallower, then  $\mathcal{F}$  could be as high as  $1/2$  or lower. Therefore, this effect could be diminished by  $\sim 1\text{--}50\%$  based on the eccentricity distribution of the comets. However,  $\sim 1\%$  accretion efficiencies could still enrich small planets with a mass of cometary material comparable to their own mass. It is possible that by comparing planetary and stellar metallicities, we will be able to estimate the amount of cometary enrichment that a given planet experienced and therefore the extent to which the measured molecular abundances are primordial.

The detection and compositional characterization of future interstellar comets will greatly refine the calculations and estimates presented in this Letter. The carbon-to-oxygen ratio of the volatile coma of an interstellar comet can be used to infer its formation location within the protostellar disk relative to the CO snow line (Seligman et al. 2022). The fraction of interstellar comets that formed exterior and interior to the CO snow line will also represent the fraction of exoplanetary enriching comets that formed in these regions.

JWST will provide measurements of elemental molecular abundances and abundance ratios in these exoplanet atmospheres (e.g., JWST Cycle 1 approved programs; Bean et al. 2018; Desert et al. 2021; Hu & Damiano 2021; Mansfield et al. 2021; Mann et al. 2021; Min et al. 2021; Stolker et al. 2021). With these observations scheduled within the next year, it will be of vital importance to quantify the effects of cometary enrichment on these exoplanets. It is feasible that this enrichment could have provided a nonnegligible fraction of the atmospheric metal content.

We thank Fred Ciesla, Megan Mansfield, Jacob Bean, Rafael Luque, Eliza Kempton, Samuel Cabot, Dan Fabrycky, Sebastián Marino, Quentin Kral, and Mark Wyatt for useful suggestions. We thank the anonymous reviewer for extremely insightful comments and constructive suggestions that greatly strengthened the scientific content of this manuscript.

J.B. has been supported by the Heising-Simons 51 Pegasi b postdoctoral fellowship. A.D.F. acknowledges support by the National Science Foundation Graduate Research Fellowship Program under grant No. (DGE-1746045). L.A.R. gratefully acknowledges support from the Research Corporation for Science Advancement through a Cottrell Scholar Award.

This research has made use of the NASA Exoplanet Archive, which is operated by the California Institute of Technology, under contract with the National Aeronautics and Space Administration under the Exoplanet Exploration Program. This research also has made use of NASA's Astrophysics Data System.

Facility: Exoplanet Archive.

### ORCID iDs

Darryl Z. Seligman  <https://orcid.org/0000-0002-0726-6480>  
 Juliette Becker  <https://orcid.org/0000-0002-7733-4522>  
 Fred C. Adams  <https://orcid.org/0000-0002-8167-1767>  
 Adina D. Feinstein  <https://orcid.org/0000-0002-9464-8101>  
 Leslie A. Rogers  <https://orcid.org/0000-0003-0638-3455>

### References

- Bailey, B. L., & Malhotra, R. 2009, *Icar*, **203**, 155  
 Bean, J. L., Stevenson, K. B., Batalha, N. M., et al. 2018, *PASP*, **130**, 114402  
 Bodewits, D., Noonan, J. W., Feldman, P. D., et al. 2020, *NatAs*, **4**, 867  
 Brasser, R., & Wang, J. H. 2015, *A&A*, **573**, A102  
 Carusi, A., Valsecchi, G. B., & Greenberg, R. 1990, *CeMDA*, **49**, 111  
 Chen, J., & Kipping, D. 2017, *ApJ*, **834**, 17  
 Cordiner, M. A., Milam, S. N., Biver, N., et al. 2020, *NatAs*, **4**, 861  
 Čuk, M. 2018, *ApJL*, **852**, L15  
 Desch, S. J., & Jackson, A. P. 2021, *JGRE*, **126**, e06706  
 Desert, J.-M., Adhiambo, V., Barat, S., et al. 2021, The nature, origin, and fate of two planets of a newborn system through the lens of their relative atmospheric properties, JWST Proposal. Cycle 1, #2149  
 Di Sisto, R. P., & Brunini, A. 2007, *Icar*, **190**, 224  
 Di Sisto, R. P., Fernández, J. A., & Brunini, A. 2009, *Icar*, **203**, 140  
 Do, A., Tucker, M. A., & Tonry, J. 2018, *ApJL*, **855**, L10  
 Duncan, M., Quinn, T., & Tremaine, S. 1988, *ApJL*, **328**, L69  
 Edgeworth, K. E. 1943, *JBAA*, **53**, 181  
 Fernandez, J. A. 1980, *MNRAS*, **192**, 481  
 Fernández, J. A. 2005, *Comets—Nature, Dynamics, Origin and their Cosmological Relevance*, Vol. 328 (Berlin: Springer)  
 Fernández, J. A., Helal, M., & Gallardo, T. 2018, *P&SS*, **158**, 6  
 Füglistaler, A., & Pfenniger, D. 2018, *A&A*, **613**, A64  
 Gomes, R. S., Morbidelli, A., & Levison, H. F. 2004, *Icar*, **170**, 492  
 Hahn, G., & Bailey, M. E. 1990, *Natur*, **348**, 132  
 Hahn, J. M., & Malhotra, R. 1999, *AJ*, **117**, 3041  
 Hands, T. O., & Helled, R. 2022, *MNRAS*, **509**, 894  
 Hansen, B., & Zuckerman, B. 2017, *RNAAS*, **1**, 55  
 Hu, R., & Damiano, M. 2021, Deep Characterization of the Atmosphere of a Temperate Sub-Neptune, JWST Proposal. Cycle 1, #2372  
 Jackson, A. P., & Desch, S. J. 2021, *JGRE*, **126**, e06807  
 Jackson, A. P., Tamayo, D., Hammond, N., Ali-Dib, M., & Rein, H. 2018, *MNRAS*, **478**, L49  
 Jewitt, D., Luu, J., Rajagopal, J., et al. 2017, *ApJL*, **850**, L36  
 Kral, Q., Wyatt, M. C., Triaud, A. H. M. J., et al. 2018, *MNRAS*, **479**, 2649  
 Kuiper, G. P. 1951, *PNAS*, **37**, 1  
 Laughlin, G., & Batygin, K. 2017, *RNAAS*, **1**, 43  
 Lellouch, E., Paubert, G., Moreno, R., et al. 1995, *Natur*, **373**, 592  
 Leonard, F. C. 1930, *ASPL*, **1**, 121  
 Levine, W. G., Cabot, S. H. C., Seligman, D., & Laughlin, G. 2021, *ApJ*, **922**, 39  
 Levine, W. G., & Laughlin, G. 2021, *ApJ*, **912**, 3  
 Levison, H. F. 1996, in *ASP Conf. Ser. 107, Completing the Inventory of the Solar System*, ed. T. Rettig & J. M. Hahn (San Francisco, CA: ASP), 173  
 Levison, H. F., & Duncan, M. J. 1997, *Icar*, **127**, 13  
 Levison, H. F., Morbidelli, A., Van Laerhoven, C., Gomes, R., & Tsiganis, K. 2008, *Icar*, **196**, 258  
 Line, M. R., Brogi, M., Bean, J. L., et al. 2021, *Natur*, **598**, 580  
 Mann, A. W., Gao, P., Kraus, A. L., et al. 2021, The Atmosphere of a 17Myr Old Hot Jupiter, JWST Proposal. Cycle 1, #2498  
 Mansfield, M., Bean, J. L., Kempton, E. M. R., et al. 2021, Constraining the Atmosphere of the Terrestrial Exoplanet Gl486b, JWST Proposal. Cycle 1, #1743  
 Marino, S., Bonsor, A., Wyatt, M. C., & Kral, Q. 2018, *MNRAS*, **479**, 1651  
 Matter, A., Guillot, T., & Morbidelli, A. 2009, *P&SS*, **57**, 816  
 Meech, K. J., Weryk, R., Micheli, M., et al. 2017, *Natur*, **552**, 378  
 Micheli, M., Farnocchia, D., Meech, K. J., et al. 2018, *Natur*, **559**, 223  
 Min, M., Bitsch, B., Bouwman, J., et al. 2021, Mineral clouds in the atmosphere of the hot Jupiter HD189733b, JWST Proposal. Cycle 1, #2001  
 Morbidelli, A., Levison, H. F., Tsiganis, K., & Gomes, R. 2005, *Natur*, **435**, 462  
 Moro-Martín, A. 2018, *ApJ*, **866**, 131  
 Moro-Martín, A. 2019, *AJ*, **157**, 86  
 Napier, K. J., Adams, F. C., & Batygin, K. 2021, *PSJ*, **2**, 53  
 Nesvorný, D., Vokrouhlický, D., Dones, L., et al. 2017, *ApJ*, **845**, 27  
 Noll, K. S., McGrath, M. A., Trafton, L. M., et al. 1995, *Sci*, **267**, 1307  
 Öberg, K. I., Murray-Clay, R., & Bergin, E. A. 2011, *ApJL*, **743**, L16  
 Podolak, M., Haghighipour, N., Bodenheimer, P., Helled, R., & Podolak, E. 2020, *ApJ*, **899**, 45  
 Quinn, T., Tremaine, S., & Duncan, M. 1990, *ApJ*, **355**, 667  
 Rafikov, R. R. 2018, *ApJ*, **861**, 35  
 Raymond, S. N., Armitage, P. J., & Veras, D. 2018, *ApJL*, **856**, L7  
 Raymond, S. N., Kaib, N. A., Armitage, P. J., & Fortney, J. J. 2020, *ApJL*, **904**, L4  
 Ruffio, J.-B., Konopacky, Q. M., Barman, T., et al. 2021, *AJ*, **162**, 290  
 Seligman, D., & Laughlin, G. 2020, *ApJL*, **896**, L8  
 Seligman, D. Z., Kratter, K. M., Levine, W. G., & Jedicke, R. 2021a, *PSJ*, **2**, 234  
 Seligman, D. Z., Levine, W. G., Cabot, S. H. C., Laughlin, G., & Meech, K. 2021b, *ApJ*, **920**, 28  
 Seligman, D. Z., Rogers, L. A., Cabot, S. H. C., et al. 2022, arXiv:2204.13211  
 Shibata, S., Helled, R., & Ikoma, M. 2020, *A&A*, **633**, A33  
 Shibata, S., Helled, R., & Ikoma, M. 2022, *A&A*, **659**, A28  
 Shibata, S., & Ikoma, M. 2019, *MNRAS*, **487**, 4510  
 Shoemaker, C. S., Shoemaker, E. M., Levy, D. H., et al. 1993, *IAU Circ.*, **5725**, 1  
 Stolker, T., Girard, J., Hinkley, S., et al. 2021, Unveiling formation signatures in the atmosphere of beta Pictoris c, JWST Proposal. Cycle 1, #2297

- Tiscareno, M. S., & Malhotra, R. 2003, [AJ](#), **126**, 3122
- Trilling, D. E., Mommert, M., Hora, J. L., et al. 2018, [AJ](#), **156**, 261
- Trilling, D. E., Robinson, T., Roegge, A., et al. 2017, [ApJL](#), **850**, L38
- Tsiganis, K., Gomes, R., Morbidelli, A., & Levison, H. F. 2005, [Natur](#), **435**, 459
- Wang, J., Wang, J. J., Ma, B., et al. 2020, [AJ](#), **160**, 150
- Weaver, H. A., A'Hearn, M. F., Arpigny, C., et al. 1995, [Sci](#), **267**, 1282
- Wyatt, M. C., Bonsor, A., Jackson, A. P., Marino, S., & Shannon, A. 2017, [MNRAS](#), **464**, 3385
- Wyatt, M. C., Kral, Q., & Sinclair, C. A. 2020, [MNRAS](#), **491**, 782
- Zhang, Y., & Lin, D. N. C. 2020, [NatAs](#), **4**, 852
- Zhou, J.-L., & Lin, D. N. C. 2007, [ApJ](#), **666**, 447
- Zwart, P. S., Torres, S., Pelupessy, I., Bédorf, J., & Cai, M. X. 2018, [MNRAS](#), **479**, L17